THREE-DIMENSIONAL TRANSIENT HEAT, MASS, MOMENTUM, AND SPECIES TRANSFER IN THE STORED GRAIN ECOSYSTEM: PART I. MODEL DEVELOPMENT AND EVALUATION

J. Lawrence, D. E. Maier, R. L. Stroshine

ABSTRACT. *A 3D transient heat, mass, momentum, and species transfer model for the stored grain ecosystem was developed using the finite element method. Hourly weather data such as ambient temperature and relative humidity, solar radiation, and wind speed were used as input in the model. The 3D model has different components that predict grain temperature and moisture content, dry matter loss, insect population, and species (CO_2 and fumigant) concentration. The 3D model was evaluated using linear elements with three different numbers of nodes and quadratic elements with three different numbers of nodes. The accuracy of prediction for each category was evaluated using the observed and predicted temperature values. The linear model with 384 nodes and the quadratic model with 415 nodes were found to be the best based on the lowest standard error compared to other combinations. Four different time discretization schemes were used to evaluate model accuracy over time. The Crank-Nicolson time discretization scheme was found to be the best of the four.*

Keywords. *3D model, Finite element method, Heat, Mass, Momentum, Species, Stored grain ecosystem.*

Grain storage is an important link in the food grain production and supply system. The factors influencing grain deterioration during storage are grain moisture content, temperature, insects, mites, molds, geographical location, and bin structural orientation (Jayas, 1995). During grain storage, temperature, moisture, and CO_2 concentration vary depending on the physical, chemical, and biological activities inside the grain bin. Temperature and moisture content of grain change due to solar radiation, natural convection, forced convection by aeration, and insect and mold activity. CO_2 concentration increases due to the biological activity of insects, molds, and grain. Insect and mold activity will lead to self-heating of the grain mass often in localized areas called "hot spots." The stored grain ecosystem is a complex domain that includes physical, chemical, and biological systems. Managing the stored grain ecosystem is very challenging. It requires an integrated management approach that combines engineering, ecological, and economic principles to prevent and solve problems. Generally, managers and producers use their past experience as a tool in managing stored grain. This approach is not scientific and sometimes leads to economic loss due to poor management. Grain shrinkage due to moisture loss is one of the main economic losses in the grain storage industry. Profit from grain storage is highly dependent upon how effectively grain moisture is managed. If moisture is lowered well below the maximum level accepted by the market without a discount or drying charge, an economic loss occurs due to excessive loss in weight. If the moisture level is above the safe limit or non-uniform in the bin, loss may occur due to spoilage by insects and molds. In order to manage stored grain effectively, site-specific management strategies such as aeration and integrated pest management (IPM) need to be developed and implemented. A computer simulation model is a fast and efficient way of generating data for a specific location. A good grain storage management tool consists of a comprehensive three-dimensional heat, mass, momentum, and gas transfer model that predicts grain temperature and moisture content and takes into account solar radiation, wind effect, forced (aeration) and natural convection, and internal heat generated due to biological activity of grain, insect, and mold respiration in the grain mass. An advanced grain management tool should allow the manager to evaluate different decisions with respect to the effects on grain quality, storage time, and costs.

Temperature changes in a grain mass can be modeled as heat transfer due to conduction, convection, or a combination of both during aeration and non-aeration periods. The boundary conditions are the important parameters that influence heat, mass, and momentum transfer in stored grain. Solar radiation and convective boundary conditions increase the temperature gradient in the grain mass, which leads to natural convection development. Natural convection is the other main driving force for the transfer of heat

Submitted for review in September 2011 as manuscript number FPE 9364; approved for publication by the Food & Process Engineering Institute Division of ASABE in November 2012.

Contribution No. 12-086-J from the Kansas Agricultural Experiment Station.

The authors are **Johnselvakumar Lawrence, ASABE Member,** Post-Doctoral Fellow, and **Dirk E. Maier, ASABE Member,** Professor and Head, Department of Grain Science and Industry, Kansas State University, Manhattan, Kansas; and **Richard L. Stroshine, ASABE Member,** Professor, Department of Agricultural and Biological Engineering, Purdue University, West Lafayette, Indiana. **Corresponding author:** Dirk E. Maier, Department of Grain Science and Industry, 201 Shellenberger Hall, Kansas State University, Manhattan, KS 66506; phone: 785-532-4052; e-mail: dmaier@ksu.edu.

  ISSN 2151-0032

and moisture in the grain mass during the non-aeration period. During aeration (forced convection), convective heat and moisture transfer are dominant. Conduction and diffusion equations are used to model both the aeration and non-aeration scenarios.

Most models related to grain storage were developed based on simplified unrealistic boundary conditions without considering solar radiation and wind effects (Thompson, 1972; Nguyen, 1987; Singh et al., 1993). The pioneers in the development of a model with realistic boundary conditions were Montross et al. (2002). They developed a 2D model with realistic boundary conditions to predict grain temperature and moisture. One limitation in the Montross model was that the important solar radiation boundary condition could not be applied properly in a 2-D model due to its non-uniformity around the bin perimeter. The degree of variation of solar radiation depends upon the solar azimuth angle around the bin. The solar azimuth angle starts from zero in the south and reaches 180° in the north direction. As a result of the earth's orientation, in the Northern Hemisphere the south side will receive maximum solar radiation and the opposite will be true in the Southern Hemisphere. Likewise, the north side of the bin in the Northern Hemisphere will receive less solar radiation than the south side.

During non-aeration, temperature gradients develop in the grain mass due to variation in ambient conditions. This leads to natural convection. Most models assumed natural convection heat transfer and assumed confined fluid flow during non-aerated storage. These assumptions are applicable only for hermetic storage and are not realistic for grain storage structures with plenum and headspace vents and eave openings. The main limitations of the 2D models are implementation of 3D variations of solar radiation heat flux around the bin, identification of the 3D location of hot spots in the grain mass, and effectiveness of fumigation movement. Three-dimensional heat transfer models for cylindrical bin domains were developed by Alagusundaram et al. (1990), Andrade et al. (2002), and Jian et al. (2005). Singh et al. (1993) developed a 3D heat, mass, and momentum transfer model for a rectangular domain. They assumed no heat loss in some boundary sections (unrealistic) for natural convection heat transfer, impermeable boundaries around the bin for momentum transfer, and no solar radiation heat flux. The Alagusundaram and Jian models used structured linear and quadratic element to mesh the cylindrical domain. This led to 3D elements with a poor aspect ratio around the boundaries. They assumed: (1) heat transfer in the grain mass was only by conduction, and (2) no natural convection currents developed during the non-aerated storage period. They used solar radiation heat flux directly on the grain mass, neglecting the bin material. If the bin material, e.g., galvanized iron (GI), was taken into consideration, the one-hour time step used in their model could not be used to predict the wall temperature. The thermal conductivity difference between the grain and the bin material (GI) leads to a non-homogenous element problem that is very complex to solve. Two separate models (one for the grain mass and the other for the bin wall) can be used to overcome these difficulties. In addition, most models did not consider the internal heat generated by respiration of insects and mold. Modeling the heat of respiration is very complex. Jia et al. (2000) simulated the internal heat generation using an artificial heat generator (electric heater) placed inside the grain mass.

Although a number of modeling approaches have been described in the literature, a comprehensive 3-D heat, mass, momentum, and species transfer model for the stored grain ecosystem driven by realistic boundary conditions has not yet been developed. Therefore, the objective of this study was to develop a comprehensive 3D finite element model for the stored grain ecosystem.

MODEL DEVELOPMENT

HEAT TRANSFER MODEL

One of the key components of a comprehensive 3D ecosystem model is the heat transfer in the grain mass. The driving force for heat transfer is the temperature gradient developed throughout the grain mass due to the effects of ambient temperature, solar radiation, and wind. The temperature gradient induces natural convection currents of varying speeds that also transfer heat by convection. The governing equation used to model 3D heat transfer due to conduction and convection given in equation 1 was based on Khankari et al. (1995), except the heat generation term:

$$(\rho_{bulk} c_{bulk})\frac{\partial T}{\partial t} + (\rho_a c_a) u_j \frac{\partial T}{\partial x_j} = \frac{\partial}{\partial x_j}\left(k_{bulk}\frac{\partial T}{\partial x_j}\right) + \rho_{bulk} h_{fg}\frac{\partial M}{\partial t} + Q_h \quad (1)$$

where j =1, 2, and 3, representing the three dimensions.

The first term on the left side represents the energy stored at a specified period of time, and the second term represents energy transfer due to convection. The first term on the right side represents the energy transfer due to conduction (Fourier law of heat conduction), and the second term represents energy liberated due to evaporation for a specific period of time. The third term represents the internal heat generated due to biological activity of insects and molds.

MASS TRANSFER MODEL

The second component in the comprehensive 3D ecosystem model is the mass transfer in the grain mass. The driving forces for moisture transfer during the non-aeration period are temperature gradient, moisture gradient (vapor pressure gradient), and natural convection. However, during the aeration period, the mass transfer is due to forced convection created by a fan. The governing equation used to model 3D mass transfer in the grain mass given in equation 2 was based on Khankari et al. (1995), except the moisture generation term:

$$\rho_{bulk}\frac{\partial M}{\partial t}+\left(\frac{\sigma}{R_v T_{ab}}\right)u_j\frac{\partial M}{\partial x_j}= \frac{\partial}{\partial x_j}\left(D_M\frac{\partial M}{\partial x_j}\right)+\frac{\partial}{\partial x_j}\left(D_T\frac{\partial T}{\partial x_j}\right) -\left(\frac{\omega}{R_v T_{ab}}\right)u_j\frac{\partial T}{\partial x_j}+Q_m \quad (2)$$

where $$D_M=\frac{D_{eff}\sigma}{T_{ab}},\ D_T=\frac{D_{eff}\omega}{T_{ab}},\ \text{and}\ D_{eff}=\frac{D_v\varepsilon}{R_v\tau} \quad (3)$$

The first term on the left side represents the moisture stored at a specified period of time, and the second term represents moisture transfer due to convection. The first term on the right side represents the moisture transfer due to diffusion, and the second and third terms represent moisture transfer caused by heat diffusion and convection, respectively. The fourth term represents the internal moisture generation due to respiration.

Momentum Transfer Model (Natural Convection)

The third component in the comprehensive 3D ecosystem model is the momentum (air velocity) transfer in the grain mass. The momentum transfer component is divided into two parts: aeration (forced convection) and non-aeration (natural convection). The 3D momentum transfer equations for incompressible flow through porous media due to natural convection are based on vorticity and the vector potential relationship (Singh et al., 1993). The mass balance in the control volume is described in the continuity equation (eq. 4). The porous media velocity loss based on Darcy's law is given in equation 5. The velocity fields are converted into a vector potential (ψ in eq. 6) and are then calculated by solving equation 7, which is the momentum equation in terms of vector potential, and using equation 8. In order to simplify the solution process, no slip boundaries were assumed throughout the domain:

$$\nabla\cdot v=0 \quad (4)$$

$$v=-\frac{K}{\mu}\left(\nabla p-\rho_f g\right) \quad (5)$$

$$v=\nabla\times\psi \quad (6)$$

$$\nabla^2\psi=-\frac{K}{\mu}\beta_t g\nabla T \quad (7)$$

$$u_1=\frac{\partial\psi_3}{\partial x_2}-\frac{\partial\psi_2}{\partial x_3},\ u_2=\frac{\partial\psi_1}{\partial x_3}-\frac{\partial\psi_3}{\partial x_1},\ u_3=\frac{\partial\psi_2}{\partial x_1}-\frac{\partial\psi_1}{\partial x_2} \quad (8)$$

Momentum Transfer Model (Forced Convection)

During the forced convection process, uniform and non-uniform velocity field scenarios were used. For uniform velocity, the prescribed velocity fields in the direction of motion were used on all nodes. Uniform velocity was calculated using the airflow capacity of a fan with static air pressure caused by airflow resistance due to the depth of the grain mass. For non-uniform velocity, the procedure described by Garg (2005) was used. However, the linear porosity variations were implemented from the center (low values) to walls (higher values) of the bin, which was different from Garg (2005). The lower porosity values were due to broken grain and fine material accumulation in the center volume of the grain mass because of particle segregation during loading. The higher bulk density particles tend to stay near the center, while lower bulk density particles move toward the wall. FLUENT was used to determine the non-uniform velocities by varying the coefficient of airflow resistance of the grain mass using Ergun's equation based on porosity. The predicted velocities were then interpolated into nodal velocities of the 3D finite element model.

Species Transfer Model

The fourth component in the comprehensive 3D ecosystem model is species (e.g., CO_2, fumigant) transfer in the grain mass. The driving forces for gas movement are convection currents (natural or forced) and concentration gradient (diffusion) in the grain mass. The governing equation for species (CO_2 or fumigant) movement inside a grain mass is given by equation 9 (Alagusundaram et al., 1996):

$$\frac{\partial C}{\partial t}+u_i\nabla C=D_s\nabla^2 C+S \quad (9)$$

where the first term on the left side represents the accumulation of gas concentration over time, and the second term represents the convection gas transfer. The first term on the right side represents the gas transfer due to diffusion, and the second term represents gas generation due to biological activity of insects and molds. Solution of this equation is subject to boundary conditions such as a concentration flux, the specified concentration, and the initial conditions such as zero concentration at time t = 0. Shunmugam et al. (2005) experimentally found the diffusion coefficients of CO_2 for wheat (5.9×10^{-6} to 7.6×10^{-6}), barley (5.1×10^{-6} to 8.4×10^{-6}), and canola (3.7×10^{-6} to 5.3×10^{-6}). Singh et al. (1993) used 0.5×10^{-5} m^2 s^{-1} as the diffusion coefficient for phosphine in corn.

Internal Heat Generation

Molds

Heat in the grain mass is generated due to biological activity, such as respiration of grains, insects, and molds. High grain moisture and temperature cause greater mold activity, which will generate more CO_2 compared to low-moisture grain. Calculation of internal heat generation (J m^{-3}) was based on heat produced due to the evolution of CO_2 when carbohydrates are broken down by microorganisms. The amount of CO_2 evolution in this model was determined using the Steele formula given in equation 10 (Thompson, 1972):

$$y=1.3\left[\exp(0.006t)-1\right]+0.015t \quad (10)$$

where shelled corn storage time in hours (t in eq. 11) was calculated using corn temperature, moisture content, kernel mechanical damage, genetic resistance to storage fungi, and fungicide treatment (*ASABE Standards*, 2005):

$$t = 9.583 M_T M_M M_D M_H M_F / 24 \quad (11)$$

Calculation of the different multipliers described in equation 11 was based on ASABE Standard D535 (*ASABE Standards*, 2005). Using equations 10 and 11, the CO_2 generation was determined for the particular grain temperature and moisture content. The chemical reaction describing this internal heat generation process is given in equation 12 (Bhat, 2006):

$$C_6H_{12}O_6 + 6O_2 \rightarrow 6CO_2 + 6H_2O + \text{heat}\,(2816\,\text{kJ}) \quad (12)$$

About 2816 kJ of heat energy and 108 g of water are released for every 264 g of CO_2 produced by stored grain. Based on the generated CO_2 concentration, the heat energy released for each element was calculated. The CO_2 values were used as a source term in the gas transfer equation (eq. 9). The released heat energy values were used as a source term in the heat transfer equation (eq. 1). The released moisture values were used as a source term in the mass transfer equation (eq. 2).

Insects

Insect-induced hot spots can reach temperatures up to 38°C. After this temperature is attained, it begins to decline, as temperatures above 38°C are lethal to insects. Cofie-Agblor et al. (1996) determined that 6.38 µW was generated per insect when 5000 insects were placed in a chamber of 200 g of wheat at 15°C to 35°C and 12% to 18% moisture content. The heat was generated due to respiration of the insects. From this study, the insect population for each element in the grain mass was predicted using an insect growth model. The heat generated was calculated from the insect count in each element and added to the source term of the heat transfer equation.

BOUNDARY CONDITIONS

Heat Transfer Equations

The boundary conditions for the energy equations were heat flux due to solar radiation, convection heat transfer due to wind interacting with the roof and wall surfaces, and heat transfer through the vent, eave, and plenum openings of the storage structure. Based on the observed values of direct solar radiation, the net solar radiation heat flux stored on the bin surfaces was calculated using equation 13 (Duffie and Beckman, 2006). The net solar radiation heat flux (q_r) stored on the bin surfaces was the summation of heat flux observed by the material (q_o), heat flux from earth to bin (q_e) and sky to bin (q_s), and from direct (q_f) and diffuse radiation (q_d):

$$q_r = q_o + q_e + q_s + q_f + q_d \quad (13)$$

The equations used to find declination, angle of incidence for beam radiation, ratio of beam radiation on a tilted surface to that on a horizontal surface, extraterrestrial radiation on a horizontal surface for an hour period, hourly clearness index, beam radiation, total solar radiation on the tilted surface for an hour, sky radiation heat flux, direct and diffuse solar radiation heat flux, earth to storage structure radiation heat flux, and storage structure to surrounding radiation heat flux are given by Duffie and Beckman (2006) and are described in detail by Lawrence (2010). The heat transfer coefficient for the convective heat transfer between the wind and the surfaces was calculated from wind speed. The viscosity and thermal conductivity of air were calculated from ambient temperature using equations described by Incropera and Dewitt (1996). The convective heat transfer coefficients around the wall and roof were calculated using equations described by Incropera and Dewitt (1996).

Mass Transfer Equations

No moisture transfer was assumed to occur across the wall. The air moisture to grain moisture relationship was calculated using the modified Chung-Pfost equilibrium moisture equation (Chung and Pfost, 1967). For the aeration period, the moisture content of the bottom boundary was calculated using the thin-layer drying equation (Montross et al., 2002). The resulting plenum temperature and relative humidity values were used to calculate the equilibrium moisture content of the bottom grain layer.

Momentum Transfer Equations

The boundary conditions for the momentum equations assumed no slip on all walls during aeration and non-aeration periods. For larger bins, in order to simplify the 3D vector potential formulation, an impermeable momentum transfer boundary condition was assumed over the grain surface and plenum during the non-aeration period. However, for smaller bins (e.g., the PHERC and SPREC bins), a constant air infiltration velocity of 0.0008 m s^{-1} was used as the natural convection velocity (Montross et al., 2002). This was due to the low height and low resistance to airflow in the grain mass for these smaller bins. Pressure at the top grain surface was assumed to be atmospheric.

Species Transfer Equation

The boundary conditions used for the species transfer equations were no species (CO_2 or fumigant) transfer through the walls. Species concentrations in the headspace and plenum were calculated by using the CO_2 concentration in the atmosphere during the aeration and non-aeration periods. The initial and boundary conditions used for the CO_2 species transfer model were as 0.03 g CO_2 kg^{-1} of air (ambient CO_2 concentration). For the fumigant species transfer model, perfectly sealed boundaries were assumed.

HEADSPACE, PLENUM, AND WALL MODELS

The grain storage structure consisted of a plenum and headspace, in addition to the grain mass. The plenum is a space below the perforated floor that holds the grain mass where air is pressurized by the aeration fan. It allows uniform distribution of air across the diameter and into the grain mass. The space above the grain mass is the headspace, which represents a large air volume between the grain surface and the underside of the roof. The headspace is ventilated via eave openings and roof vents. The material properties of the headspace and plenum (air) and the wall

(GI) are different from those of the grain mass. Solving equations that are used for air, grain and GI wall together is cumbersome. The boundary layer problem associated with air moving from the grain mass to the headspace and vice versa is complex in nature. The one-hour simulation time step used for the grain mass cannot be used for either the air medium or the GI material. This is due to the different thermal diffusivity properties of air, GI, and grain. Therefore, separate energy balance equations were formulated for the headspace, plenum, and wall to find the headspace air, plenum air, and wall temperatures. In addition, mass balance equations were formulated for the headspace and plenum to find the relative humidities of the headspace and plenum air. The local wind velocity near the bin vents was calculated using the following correlation between ambient wind velocity and bin height (Allocca et al., 2003):

$$V_h = 0.35 V_{met} h^{0.25} \tag{14}$$

where the input for these energy and mass balance models was the ambient temperature and RH, wind speed, and solar radiation. These energy and mass balance models were a system of ordinary differential equations and were coupled together. Details about the equations are explained by Lawrence and Maier (2011). These equations were solved using fourth-order Runge-Kutta methods. The predicted headspace, plenum, and wall temperatures were used as the prescribed boundary conditions for the energy transfer equation. The predicted headspace and plenum air humidities and temperatures were used to find the equilibrium moisture content of the particular grain, and these values were used as the prescribed boundary conditions for the mass transfer equation during non-aeration.

FINITE ELEMENT MODEL

The approximate solutions of the partial differential equations (PDE) given in equations 1, 2, 7, and 9 were determined by the finite element method (FEM) technique (Reddy, 2003). A hexahedral (brick) element shape was used to discretize the 3D domain consisting of a cylindrical bin with a grain mass. The continuous quantities (temperature, moisture, velocity, and species) were approximated over each element by using interpolating functions. The interpolating functions (linear and quadratic) were selected based on the solution to the governing equations. The Galerkin method (weighted residual) was used for formulating the PDE into finite element discrete systems of equations. These systems of equations were solved by the LU decomposition method.

Eight-node linear and 27-node quadratic brick elements were used for the formulation (fig. 1). The general form of the approximate solutions for temperature, moisture, and velocity over an element are given in equations 15 and 16. The numerical solutions were the approximate solutions expressed in equation 17. The coefficients of the interpolating functions were chosen in such a way that the residual (R) becomes zero over a chosen domain. This was achieved by integrating the residual equation with the interpolating functions expressed in equation 18. In the Galerkin weighted residual method, the weighing functions (W_m) are

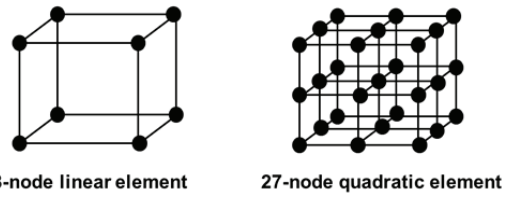

Figure 1. Element types used in the finite element formulation.

the interpolating functions (ϕ). The residual equations generated from equations 1, 2, 4, and 9 were substituted in equation 18 appropriately to form four finite element formulation equations: one each for temperature, moisture, species, and velocity. The finite element formulated equations for temperature, moisture, and species transfer are given in equations 19 through 21:

$$\bar{T}^e = \sum_{j=1}^{n} T_j \xi_j^e, \quad \bar{M}^e = \sum_{j=1}^{n} M_j \xi_j^e \tag{15}$$

$$\bar{u}^e = \sum_{j=1}^{n} u_j \xi_j^e, \quad \bar{v}^e = \sum_{j=1}^{n} v_j \xi_j^e, \quad \bar{w}^e = \sum_{j=1}^{n} w_j \xi_j^e \tag{16}$$

where $n = 8$ for a linear element and $n = 27$ for a quadratic element.

$$T \neq \bar{T}, M \neq \bar{M}, u \neq \bar{u}, v \neq \bar{v}, w \neq \bar{w} \tag{17}$$

$$\iiint W_m(x, y, z) R dx dy dz = 0 \tag{18}$$

$$\frac{\partial T_j}{\partial t}\left[C^1_{ij}\right] + \left[K^1_{ij}\right]\{T_j\} = \{F_t\} \tag{19}$$

$$\frac{\partial M_j}{\partial t}\left[C^2_{ij}\right] + \left[K^2_{ij}\right]\{M_j\} = \{F_m\} \tag{20}$$

$$\frac{\partial S_j}{\partial t}\left[C^3_{ij}\right] + \left[K^3_{ij}\right]\{S_j\} = \{F_s\} \tag{21}$$

MODEL IMPLEMENTATION

The grain storage structure model consisted of a plenum, wall, grain mass, and headspace. The wall, headspace, and plenum conditions were modeled separately using the control volume energy and mass balance approach. The wall, headspace, and plenum models are described in detail by Lawrence (2010). These models predict the headspace air, plenum air, and wall temperatures and the headspace and plenum air relative humidities. The bin domain was discretized into only one domain: the grain mass.

The accuracy of the model depends upon the number of nodes and size of the elements. The selection of nodes depends on the level of accuracy desired and reasonable computational time. Three different sizes of 8-node linear elements and three different sizes of 27-node quadratic elements were selected for evaluation of the model. The numbers of nodes were selected based on element size for both linear and quadratic mesh. The element edge length ranged from 0.06 to 0.15 m for the linear and quadratic

Table 1. Linear and quadratic elements with number of nodes and elements used in the 3D model simulations.

Element Type	Name	Nodes	Elements
Linear	L-1	384	235
	L-2	792	588
	L-3	1152	880
Quadratic	Q-1	415	36
	Q-2	805	75
	Q-3	1305	128

mesh. The details are given in table 1. The meshing of the grain mass domain with various linear and quadratic elements was done using Gambit 2.2.3 software. Numerous experimental runs were conducted with different numbers of nodes and elements to find the appropriate number of nodes and elements in terms of accuracy and computational time. Singh and Thorpe (1993) optimized the grid size for a finite difference grid by conducting numerical experiments with different element numbers using in succession 11, 20, 25, 31, 35, and 41 lateral grid points. They concluded that a grid consisting of 31 × 31 × 31 points was found sufficient for a 10 m × 20 m × 5 m corn storage bunker based on accuracy and computational time. Andrade et al. (2002) used 2169 nodes and 1728 linear elements to model a cylindrical bin with a diameter of 3.6 m and a grain height of 1.7 m using the finite element software ANSYS.

For this study, the mesh geometry information was obtained from the Gambit output file and formed a separate input file for the 3D model. The various grain and bin material properties, fan control status, weather data, initial parameters, and initial conditions were specified in files with specific extensions. The 3D finite element ecosystem model was coded in Fortran 90 using the software Compaq Visual Fortran 6.6b.

SEGREGATED SOLVER PROCEDURE

The above energy, mass, and momentum transfer governing equations are coupled. Due to the complexity of solving these coupled equations, the segregated solver approach was used. Two different sequences were used: one for aerated conditions, and the other for non-aerated conditions. For the non-aeration mode, the energy transfer equation was solved first assuming zero velocities in all three dimensions and no moisture gradient. The temperature gradient was calculated using gradient equations during post-processing. The moisture transfer equation was solved next using the calculated temperature gradient and assuming zero velocities in all three dimensions. The moisture gradient was calculated using gradient equations during post-processing. Thirdly, the momentum transfer equations were solved with the calculated temperature gradient as the driving force for the natural convection scenario. Given that the coupling of these three equations is non-linear, several iterations are required to converge to the specified accuracy. It was observed that the solutions converged to an accuracy of 0.000001 within four iterations. One and two iterations yielded accuracy levels of 0.0001 and 0.00001, respectively. Therefore, all simulations were iterated only once, taking into consideration the computational time and low accumulation of error per time step (Montross et al., 2002).

For the aeration mode, the momentum equations were solved for the forced convection scenario using Fluent software. These velocities were used in the convection terms of the energy and moisture equations to find the temperatures and moisture contents. The 3D velocities were stored and called at appropriate times for aeration. There were minimal changes in the airflow resistance within the grain bulk over time, and therefore the airflow velocity at each node will not change.

POST-PROCESSING

Insect Population

The insect population over a period of time was calculated using the Throne (1994) model. This model predicted the insect population from the survival rate for eggs that mature to become adults and the maize weevil development rate based on temperature and relative humidity. The duration of development was based on environmental conditions that were calculated based on equations given by Throne (1994). The proportion of eggs surviving to the adult stage was based on temperature and relative humidity, which were calculated based on equations given by Throne (1994). The stored grain ecosystem computer model assumed that the temperature limits of the insect development rate were between 12°C and 35°C. Outside these limits, the development rate was assumed to be zero. The insect population was calculated every day based on average daily grain temperature and relative humidity.

Dry Matter Loss

Dry matter loss of corn over a period of time was calculated using the equations given by ASABE Standard D535 (*ASABE Standards*, 2005). Dry matter loss is a function of "equivalent reference storage time," which depends on various multipliers such as temperature, moisture, damage, genetic, and fungicide. Dry matter loss was calculated for every hour for each element based on average element temperature and moisture content (Bartosik and Maier, 2004).

MODEL EVALUATION

After the model was developed, it was evaluated by running it using different numbers of nodes and elements and by using linear versus quadratic interpolation functions. The transient part of the model was evaluated using four different finite difference time-stepping schemes: Crank-Nicolson ($\theta = 0.5$), Galerkin ($\theta = 0.67$), Euler forward difference ($\theta = 0$), and Euler backward difference ($\theta = 1$) (Reddy, 2003). There are two types of heat capacity mass matrix formulations: lumped mass matrices and consistent mass matrices. In the lumped heat capacity system, there is no spatial variation of temperature. The temperature change in this system occurs only with respect to time (Lewis et al., 2004). Since the thermal conductivity of most type of grains is low (0.08 to 0.4 W m^{-1} K^{-1} depending on moisture content), the changes in temperature were also very slow. A definite temperature gradient developed within each element. Several preliminary simulations were run, and it was determined that propagation in the lumped heat capacity

system of finite element analysis was very slow. This was not a realistic result based on prior researcher studies (Muir et al., 1980; Montross et al., 2002; Jian et al., 2005). Therefore, the 3D model was evaluated only using the consistent mass matrix heat capacity formulation.

Grain temperature data collected during 1999 in Bin 12 of the Post-Harvest Education and Research Center (PHERC) located at the Agronomy Center for Research and Education (ACRE) of Purdue University were used for the evaluation of the 3D model. The temperature data over time reflect changes caused by conduction and natural convection heat transfer in the grain mass. Outputs for meshes with different numbers of nodes for the grain bin domain of Bin 12 (2.1 m grain depth and 2.7 m diameter) were compared to evaluate which one gave the highest accuracy compared to the observed values. Since an analytical solution is not possible for this conduction-convection FE model, only observed values were used to determine accuracy. The standard errors of the estimate (SE) between the predicted and observed values were calculated using equation 22 (Devore, 2007). The standard error of the estimate gives a measure of the accuracy of predictions (i.e., the mean standard deviation between the observed and predicted values):

$$SE = \sqrt{\frac{\sum (Y - Y')^2}{n}} \qquad (22)$$

Linear Element Model

Three types of linear element model (table 1) were used to evaluate the 3D stored grain ecosystem model. The predicted values were compared with observed values using the standard error of the estimate. The error analysis data for the three linear element models for the center and south locations are given in tables 2 and 3. The predicted and observed variations in grain temperature in the center of the grain mass at 0.9 m above the plenum for the L-1 model are given in figure 2, and values for the south side of the grain mass are given in figure 3. The standard error of the estimate for the three linear element models ranged between 1.7°C and 2.3°C for the center location and between 1.8°C and 3.9°C for the south location. At 0.3 m above the plenum near the south wall, the predicted values followed the path of observed values with standard errors of 1.8°C for L-1, 3.2°C for L-2, and 3.5°C for L-3. There was a major difference of 1.4°C to 1.7°C between the L-1, L-2, and L-3 models at 0.3 m above the plenum. Error values above 1.6°C for the linear element models were likely due to several factors, such as element size and time step, and not knowing the exact natural convection current moving into the bin over time during non-aeration. The accuracy of different element and node combinations depends on the element size and time step (Segerlind, 1984). A one-hour time step (i.e., 3600 s) was used in all simulations, as the boundary conditions were updated every hour. The computational time required for each simulation depends on the size of the elements and the number of nodes. For 792 nodes, a four-month simulation required eight hours. The computational time was also influenced by the type of microprocessor used. Among the three linear models, the L-1 model (384 nodes and 235 elements) predicted the most accurate results. Therefore, the L-1 model was used for validation of the 3D model for linear elements.

Table 2. Standard error of estimate (°C) for predicted versus observed grain temperatures at the center location of the grain mass above the plenum of PHERC Bin 12 during May-August 1999.

	Distance above Plenum		
Model	0.3 m	0.9 m	1.5 m
L-1	1.9	1.8	2.3
L-2	2.2	1.7	1.9
L-3	2.3	1.9	1.8
Mean	2.1	1.8	2.0
SD	0.2	0.1	0.3
Q-1	1.9	2.2	2.8
Q-2	2.4	2.1	3
Q-3	2.6	2.5	2.7
Mean	2.3	2.3	2.8
SD	0.4	0.2	0.2

Table 3. Standard error of estimate (°C) for predicted versus observed grain temperatures at the south location of the grain mass above the plenum of PHERC Bin 12 during May-August 1999.

	Distance above Plenum		
Model	0.3 m	0.9 m	1.5 m
L-1	1.8	2.3	3
L-2	3.2	3.3	3.7
L-3	3.5	3.6	3.9
Mean	2.8	3.1	3.5
SD	0.9	0.7	0.5
Q-1	1.8	1.9	2.1
Q-2	2.2	2.5	2.6
Q-3	2.4	2.5	2.7
Mean	2.1	2.3	2.5
SD	0.3	0.3	0.3

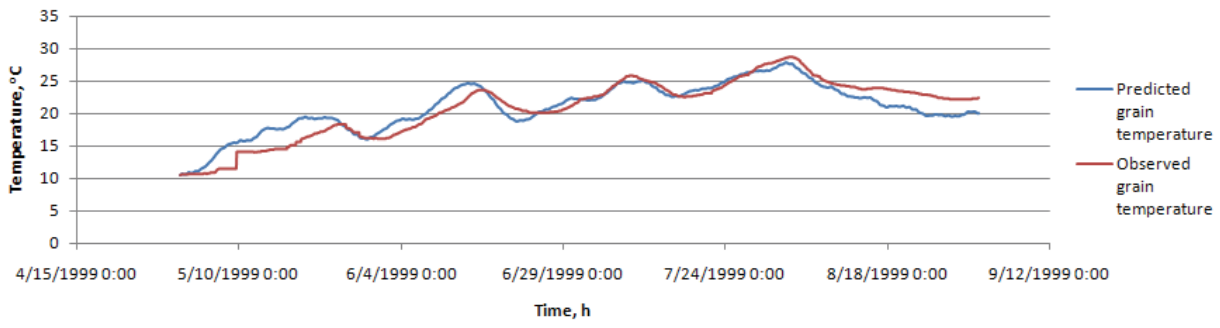

Figure 2. Grain temperature 0.9 m above the plenum in the center of the grain mass in PHERC Bin 12 during May-August 1999 for L-1.

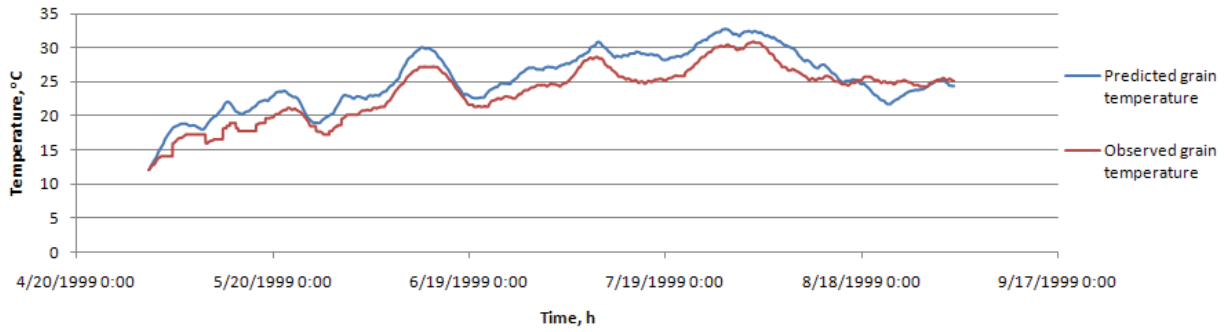

Figure 3. Grain temperature 0.9 m above the plenum on the south side of the grain mass in PHERC Bin 12 during May-August 1999 for L-1.

Quadratic Element Model

Three types of quadratic (brick) elements were used to evaluate the 3D model. The numbers of nodes and elements are given in table 1. The standard errors of the estimate for the three quadratic element models for the center and south locations are given in tables 2 and 3. The predicted and observed variations in grain temperature in the center and south locations at 0.9 m above the plenum of the grain mass for the Q-1 model are plotted in figures 4 and 5. The standard error of the estimate for the three quadratic element models ranged between 1.9°C and 3.0°C for the center location and between 1.8°C and 2.7°C for the south location. The Q-3 model predicted with the highest standard error of 2.7°C at 1.5 m above the south plenum. The Q-1 model predictions were second best and gave a standard error of 1.8°C, 1.9°C, and 2.1°C at 0.3 m, 0.9 m, and 1.5 m above the south plenum. As the element number and size increased, the standard error also increased. The error differences between the quadratic models were caused by factors such as element size and time step ratio and the physical properties of the material used.

Factors that affect the error in the linear and quadratic models were dependent on the element size, time step, material properties, and numerical oscillation caused by the convection term and wave propagation. The major difference between the linear and quadratic models is their gradient calculations. For linear models, the gradient within an element is constant; for quadratic models, the gradient varies within the elements.

Between linear and quadratic elements, linear elements predicted with lesser standard error of prediction at the center location, while quadratic elements predicted with lesser standard error at the south location. This was due to the fact that fewer elements were used in the quadratic formulation (table 1). The node and element allocation in the center location was not quite enough to carry the information, which led to higher standard error for the center location. The boundary region for the quadratic element formulation had enough nodes and elements; therefore, the standard error was less in the south location, which was close to the boundary.

Time Discretization Schemes

Four different time-stepping schemes were evaluated us-

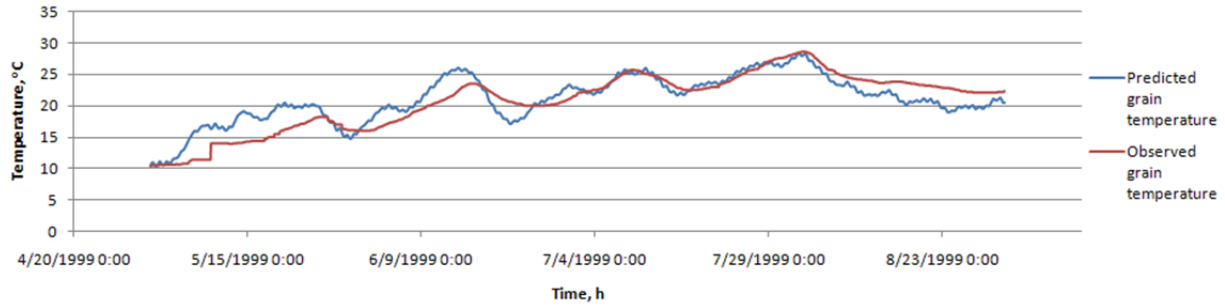

Figure 4. Grain temperature 0.9 m above the plenum near the center of the grain mass in PHERC Bin 12 during May-August 1999 for Q-1.

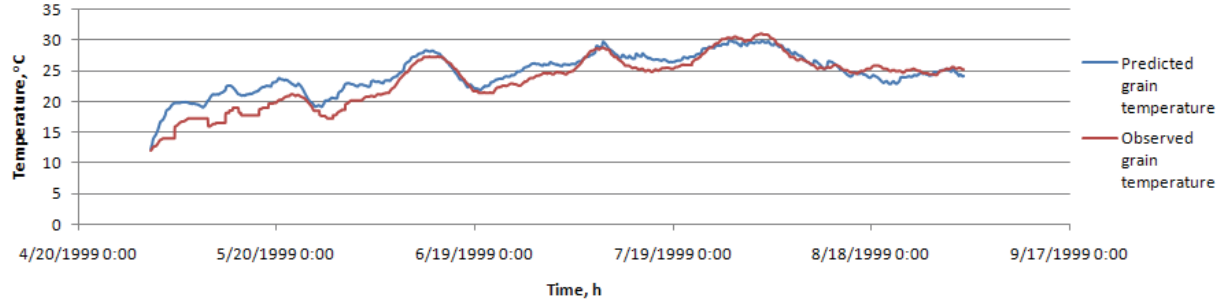

Figure 5. Grain temperature 0.9 m above the plenum near the south side of the grain mass in PHERC Bin 12 during May-August 1999 for Q-1.

Table 4. Standard error (°C) of temperature prediction at the center of the grain mass using four different time-stepping schemes.

	Distance above Plenum		
Time-Stepping Scheme	0.3 m	0.9 m	1.5 m
Euler forward difference	1.99	1.61	3.83
Crank-Nicolson	1.99	1.60	3.82
Galerkin	1.98	1.60	3.82
Euler backward difference	1.99	1.61	3.83

ing the conduction heat transfer finite element formulation. The standard errors of prediction of grain temperature at the center of the bin using each of these schemes are given in table 4. It is observed that there was no major change in the temperature prediction values for all the time-stepping schemes. The Crank-Nicolson and Galerkin schemes were slightly better than the Euler forward difference and backward difference schemes. The Crank-Nicolson scheme gives second-order accuracy in time, whereas the Galerkin scheme gives first-order accuracy in time (Yang and Gu, 2004). Therefore, the Crank-Nicolson time-stepping scheme was selected to use in the 3D model for all the simulations.

CONCLUSIONS

A three-dimensional transient heat, mass, momentum and species transfer model for the stored grain ecosystem was successfully developed using the finite element method. It allows for prediction of the grain temperature and moisture content, dry matter loss, insect population, and species (CO_2 or fumigant) concentration. The model was evaluated with respect to node and element number and type, and time discretization scheme, by comparing observed and predicted temperature values. The following are the conclusions of this study:

- The linear model with 384 nodes and 235 elements, and the quadratic model with 415 nodes and 36 elements were found to yield the lowest standard errors.
- The linear model predicted with a low standard error of 1.8°C to 2.1°C in the center location, whereas the quadratic model predicted with a low standard error of 2.1°C to 2.5°C in the south location.
- There was no significant difference in prediction of grain temperatures among the four different time-stepping schemes evaluated. The Crank-Nicolson scheme was chosen because it gives second-order accuracy with reasonable computational time.

ACKNOWLEDGEMENTS

The information contained in this publication was generated as part of a large-scale, long-term effort between Purdue University, Kansas State University, Oklahoma State University, and the USDA-ARS Center for Grain and Animal Health Research funded by the USDA-CSREES Risk Assessment and Mitigation Program (RAMP), Project No. S05035, entitled "Consortium for Integrated Management of Stored Product Insect Pests." The aim of this project is twofold: (1) to investigate and develop alternative prevention, monitoring, sampling, and suppression measures for organophosphate insecticides used directly on post-harvest grains that are under scrutiny as a result of the U.S. Food Quality Protection Act (FQPA), and (2) to find alternatives to methyl bromide, which can only be used as a fumigant for pest control in U.S. grain processing facilities under a Critical Use Exemption (CUE) as a result of the Montreal Protocol. The collaboration and participation of grain producers, handlers, and processors as well as numerous equipment and service suppliers in this project across the U.S. is greatly appreciated.

REFERENCES

Alagusundaram, K., D. S. Jayas, N. D. G. White, and W. E. Muir. 1990. Three-dimensional, finite element, heat transfer model of temperature distribution in grain storage bins. *Trans. ASAE* 33(2): 577-584.

Alagusundaram, K., D. S. Jayas, N. W. E. Muir, and D. G. White. 1996. Convective-diffusive transport of carbon dioxide through stored-grain bulks. *Trans. ASAE* 39(4): 1505-1510.

Allocca, C., Q. Chen, and L. R. Glicksman. 2003. Design analysis of single-sided natural ventilation. *Energy and Buildings* 35(8): 785-795.

Andrade, E. T., S. M. Couto, D. M. Queiroz, L. R. A. Faroni, and G. S. Damasceno. 2002. Three-dimensional simulation of the temperature variation in corn stored in metallic bin. ASAE Paper No. 023150. St. Joseph, Mich.: ASAE.

ASABE Standards. 2005. D535: Shelled corn storage time for 0.5% dry matter loss. St. Joseph, Mich.: ASABE.

Bartosik, R. E., and D. E. Maier. 2004. Evaluation of three NA/LT in-bin drying strategies in four Corn Belt locations. *Trans. ASAE* 47(4): 1195-1206.

Bhat, C. 2006. Early detection of grain spoilage and prediction of movement of low levels of CO_2 in a storage tank. MS thesis. West Lafayette, Ind.: Purdue University.

Cofie-Agblor, R., W. E. Muir, R. N. Sinha, and P. G. Fields. 1996. Heat production by adult *Crytolestes ferrugineus* (Stephens) of different ages and densities. *Postharvest Biol. Tech*. 7(4): 371-380.

Chung, D. S., and H. B. Pfost. 1967. Adsorption and desorption of water vapor by cereal grains and their products: Part I. Heat and free energy changes of adsorption and desorption. *Trans. ASAE* 10(4): 549-555.

Devore, J. L. 2007. *Probability and Statistics for Engineering and the Sciences*. Boston, Mass.: Brooks/Cole.

Duffie, J. A., and W. A. Beckman. 2006. *Solar Engineering of Thermal Processes*. Hoboken, N.J.: John Wiley and Sons.

Garg, D. 2005. Modeling non-uniform airflow and its application for partial chilled aeration using PHAST-FEM. MS thesis. West Lafayette, Ind.: Purdue University.

Incropera, F. P., and D. P. Dewitt. 1996. *Fundamentals of Heat and Mass Transfer*. Hoboken, N.J.: John Wiley and Sons.

Jayas, D. S. 1995. Mathematical modeling of heat, moisture, and gas transfer in stored-grain ecosystems. In *Stored-Grain Ecosystems*, 527-565. D. S. Jayas, N. D. White, and W. E. Muir, eds. New York, N.Y.: Marcel Dekker.

Jia, C., D. Sun, and C. Cao. 2000. Mathematical simulation of temperature fields in a stored grain bin due to internal heat generation. *J. Food Eng.* 43(4): 227-233.

Jian, F., D. S. Jayas, N. D. G. White, and K. Alagusundaram. 2005. A three-dimensional, asymmetric, transient model to predict grain temperatures in grain storage bins. *Trans. ASAE* 48(1): 263-271.

Khankari, K. K., S. V. Patankar, and R. V. Morey. 1995. A

mathematical model for natural convection moisture migration in stored grain. *Trans. ASAE* 38(6): 1777-1787.
Lawrence, J. 2010. Three-dimensional transient heat, mass, momentum, and species transfer stored grain ecosystem model using the finite element method. PhD diss. West Lafayette, Ind.: Purdue University.
Lawrence, J., and D. E. Maier. 2011. Development and validation of a model to predict air temperatures and humidities in the headspace of partially filled stored grain silos. *Trans. ASABE* 54(5): 1809-1817.
Lewis, R. W., P. Nithiarasu, and K. N. Seetharamu. 2004. *Fundamentals of the Finite Element Method for Heat and Fluid Flow.* Hoboken, N.J.: John Wiley and Sons.
Nguyen, T. V. 1987. Natural convection effects in stored grains: A simulation study. *Drying Tech.* 5(4): 541-560.
Montross, M. D., D. E. Maier, and K. Haghighi. 2002. Development of a finite-element stored grain ecosystem model. *Trans. ASAE* 45(5): 1455-1464.
Muir, W. E., B. M. Fraser, and R. N. Sinha. 1980. Simulation model of two-dimensional heat transfer in controlled-atmosphere grain bins. In *Controlled Atmosphere Storage of Grains*, 385-398. J. Shejbal, ed. Amsterdam, The Netherlands: Elsevier Scientific.
Reddy, J. N. 2003. *An Introduction to the Finite Element Method.* New York, N.Y.: McGraw-Hill.
Segerlind, L. J. 1984. *Applied Finite Element Analysis.* Hoboken, N.J.: John Wiley and Sons.
Shunmugam, G., D. S. Jayas, N. D. G. White, and W. E. Muir. 2005. Diffusion of carbon dioxide through grain bulks. *J. Stored Prod. Res.* 41(2): 131-144.
Singh, A. K., and G. R. Thorpe. 1993. A solution procedure for three-dimensional free convective flow in peaked bulks of grain. *J. Stored Prod. Res*. 29(3): 221-235.
Singh, A. K., E. Leonardi, and G. R. Thorpe. 1993. A solution procedure for the equations that govern three-dimensional free convection in bulk stored grains. *Trans. ASAE* 36(4): 1159-1173.
Thompson, T. L. 1972. Temporary storage of high-moisture shelled corn using continuous aeration. *Trans. ASAE* 15(2): 333-337.
Throne, J. E. 1994. Life history of immature maize weevils (Coleptera: Curculiondiae) on corn stored at constant temperatures and relative humidities in the laboratory. *J. Econ. Entomol.* 23(6): 1459-1471.
Yang, C., and Y. Gu. 2004. Minimum time-step criteria for the Galerkin finite element methods applied to one-dimensional parabolic partial differential equations. *Numerical Methods for Partial Differential Equations* 22(2): 259-273.

NOMENCLATURE

C = concentration of species at time t (kg m^{-3})
c_a = specific heat of air (kJ kg^{-1} K^{-1})
c_{bulk} = specific heat of bulk grain (kJ kg^{-1} K^{-1})
C_{ij} = consistent mass matrix
D_{eff} = effective diffusivity of water vapor (m^2 s^{-1})
D_s = species diffusion coefficient (m^2 s^{-1})
D_v = diffusivity of water vapor (m^2 s^{-1})
F_m = force vector for moisture equation (W m^{-3})
F_s = force vector for species equation (W m^{-3})
F_t = force vector for temperature equation (W m^{-3})
g = acceleration due to gravity (m s^{-2})
GI = galvanized iron
h = bin height (m)
h_{fg} = latent heat of vaporization (kJ kg^{-1})
k_{bulk} = bulk thermal conductivity (W m^{-1} K^{-1})
K_{ij} = conductance matrix
M = grain moisture content (kg H_2O kg^{-1} dry matter)
M_D = damage multiplier
M_F = fungicide multiplier
M_H = hybrid resistance multiplier
M_M = moisture multiplier
M_T = temperature multiplier
n = number of data points
p = vapor pressure (Pa)
Q_h = internal heat generation (J m^{-3})
Q_m = internal moisture generation due to respiration (kg m^{-3})
R = residual for moisture equation in FEM formulation
R_v = vapor pressure gas constant (J kg^{-1} °C^{-1})
S = amount of species produced by biological or chemical activity in the grain mass (kg m^{-3} s^{-1})
t = time (s) in equations 1, 2, 7, 9, 19, 20, and 21
t = shelled corn storage time for 0.5% dry matter loss (h) in equations 10 and 11
T = temperature (°C or K)
T_{ab} = absolute temperature (K)
u = air velocity in x direction (m s^{-1})
u_i = velocity of species (m s^{-1}; i = 1, 2, and 3)
u_j = jth component of air velocity (m s^{-1}; j = 1, 2, and 3)
v = air velocity in y direction (m s^{-1})
V_h = local wind velocity at specified bin height h (m s^{-1})
V_{met} = meteorological wind speed (m s^{-1})
w = air velocity in z direction (m s^{-1})
y = CO_2 produced (g CO_2 kg^{-1} dry matter)
Y = observed data
Y' = predicted data

GREEK LETTERS

β_t = coefficient of thermal expansion (K^{-1})
ε = porosity (decimal)
κ = permeability of air in porous grain (m^2 s^{-1})
μ = dynamic viscosity of air (Pa s)
ν = kinematic viscosity of air (m^2 s^{-1})
ρ_a = density of air (kg m^{-3})
ρ_{bulk} = bulk density of grain (kg m^{-3})
ρ_f = density of air (kg m^{-3})
σ = vapor pressure with respect to moisture gradient ($\sigma = \partial p_v/\partial M$)
τ = tortuosity
ψ = vector potential function
ω = vapor pressure with respect to temperature gradient ($\omega = \partial p_v/\partial T$)